Steel and Composite Structures, *Vol. 34, No. 3 (2020) 393-407*
DOI: https://doi.org/10.12989/scs.2020.34.3.393

The effect of RBS connection on energy absorption in tall buildings with braced tube frame system

Mahdi Shariati[1,2a], Mostafa Ghorbani[3b], Morteza Naghipour[3c], Nasrollah Alinejad[3d] and Ali Toghroli[*4]

[1]*Division of Computational Mathematics and Engineering, Institute for Computational Science, Ton Duc Thang University, Ho Chi Minh City, Vietnam*
[2]*Faculty of Civil Engineering, Ton Duc Thang University, Ho Chi Minh City, Vietnam*
[3]*Department of Civil, Babol Noshirvani University of Technology, Babol, Iran*
[4]*Institute of Research and Development, Duy Tan University, Da Nang 550000, Viet Nam*

(*Received August 17, 2019, Revised November 27, 2019, Accepted December 1, 2019*)

Abstract. The braced tube frame system, a combination of perimeter frame and bracing frame, is one of the systems used in tall buildings. Due to the implementation of this system in tall buildings and the high rigidity resulting from the use of general bracing, providing proper ductility while maintaining the strength of the structure when exposing to lateral forces is essential**.** Also, the high stress at the connection of the beam to the column may cause a sudden failure in the region before reaching the required ductility. The use of Reduced Beam Section connection (RBS connection) by focusing stress in a region away from beam to column connection is a suitable solution to the problem. Because of the fact that RBS connections are usually used in moment frames and not tested in tall buildings with braced tube frames, they should be investigated. Therefore, in this research, three tall buildings in height ranges of 20, 25 and 30 floors were modeled and designed by SAP2000 software, and then a frame in each building was modeled in PERFORM-3D software under two RBS-free system and RBS-based system. Nonlinear time history dynamic analysis is used for each frame under Manjil, Tabas and Northridge excitations. The results of the Comparison between RBS-free and RBS-based systems show that the RBS connections increased the absorbed energy level by reducing the stiffness and increasing the ductility in the beams and structural system. Also, by increasing the involvement of the beams in absorbing energy, the columns and braces absorb less energy.

Keywords: tall building; braced tube frame; energy absorption; RBS connections

1. Introduction

The rapid growth of population and the human need for a place to settle, along with the advances of science and the reduction of built-up land in cities, led designers to the tall buildings. Generally, the height of the structure is a relative state, and the buildings cannot be classified according to the height or number of their floors. From the engineering point of view, a building can be named as a tall building, when lateral forces caused by wind and earthquakes have a significant impact on its design procedure. In this regard, tall buildings have different lateral behavior and a special lateral system should be considered for design of these buildings. These lateral systems include rigid moment frame, braced frame, frame with belt hold, perimeter frame, enclosed perimeter frame, and braced tube frame (Yoo *et al.* 2008, Bazzaz *et al.* 2015, Khorami *et al.* 2017a, Khorami *et al.* 2017b). The braced tube frame, which is a combination of a perimeter frame and a bracing frame, due to the presence of multi-floors lateral restraints on rigid frames of the building's perimeter and as a result, the high stiffness of the lateral system, meets the need for high stiffness and resistance in tall buildings and thus increase the efficacy of structural system in order to heighten the altitude of the buildings. The braced tube frame is known as a truss tube system, in which gravity loads and lateral forces are tolerated by beams, columns and restraints. This system was first used in 1969 at the steel structure of Jon Hongkok in Chicago, and later in New York City on 1989 at 780 concrete building which is located at 3rd New York Street. In Fig. 1, the braced tube frame is shown (Shariati 2008, Thai *et al.* 2012).

In this system, the presence of general restraints on the rigid perimeter frames has a great influence on the stiffness and strength of the structure and by increasing the strength of the structure, it can reduce energy absorption and the ductility of the system, which is not desirable when encountering the earthquake lateral forces (Jeong *et al.* 2006). Also, the high stress at the connection of the beam to the column causes failure in the area before the structure

*Corresponding author, Ph.D.
E-mail: alitoghroli@duytan.edu.vn
[a]Ph.D.
E-mail: shariati@tdtu.edu.vn
[b]MSC.
E-mail: ar_mostafa_civil89@yahoo.com
[c]Professor
E-mail: m.naghi@nit.ac.ir
[d]MSC.
E-mail: nas.alinejad@gmail.com

ISSN: 1229-9367 (Print), 1598-6233 (Online)

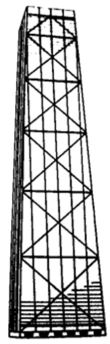

Fig. 1 A tall building with braced tube frame lateral system

reaches the final ductility (Heydari *et al.* 2018). The proposed solution for the problem is using RBS connection. This connection removes the tension from the connection point by reducing the cross section at a specific location of the beam, and this will affect the energy absorption process and, consequently, the ductility of structure, which should be studied. This connection has been studied by a number of researchers in the moment frame, which is reviewed below. A research by (Shen *et al.* 2000) experimented the seismic performance of moment frames by RBS connection and introduced the design issue. They studied dynamic time history and nonlinear static analyzes of RBS connections in 8 frames with 3-story and 10-story and discussed the function of the frame in plastic displacement sections, non-elastic drift, resistance requirements, and quantitative indexes such as flange reduction and RBS connection location. A study by (Ghassemieh *et al.* 2013) in 2012 investigated the seismic performance of RBS connection on the story drift and shear deformation in panel zones. They indicated that flexibility of this kind of connection leads to a reduction in shear demand and distortion of panel zones. In 2006, (Kassegne 2007) studied steel moment resisting frames following the 1994 earthquake in Northridge and Kobe 1995, due to brittle failure of the beam-column connection. He examined the effect of the RBS connection and expressed his research results in ordinary moment resisting frames (OMRF). In some recherches by (Sun *et al.* 2011, Khorami *et al.* 2017c, Khorramian *et al.* 2017, Li *et al.* 2019, Sajedi *et al.* 2019) expressed analytical equations and hysteretic models for different kind of braces. A research by (Yoo *et al.* 2008) studied the special bracing frames in 2007 and investigated the effect of connection design parameters on the seismic performance of bracing frames, but their studies were not based on tall structures, nor on braced tube frames. In 1995, (Vafai *et al.* 1995) analyzed 16 frames with single diagonal or X-type braces. Their results show that using single diagonal brace system reduces the general deflection of the tall building and the reduction increases as the height of the building increases. In 2008, (Fan *et al.* 2009, Shah *et al.* 2016a, Shah *et al.* 2016b, Shariat *et al.* 2018, Milovancevic *et al.* 2019, Sajedi and Shariati 2019, Shariati *et al.* 2019) studied the Taipei 101 floors building in China, and, referring to the reduced section, after modeling and testing, the seismic response was numerically investigated, then the lateral displacements and the distribution of internal column forces under time history analysis were obtained. Finally, they extracted the elastic and in-elastic response. But the systems studied were a steel-concrete composite system with a steel bracing core with a truss belt. In the same year, Sang-Whan Han and colleagues pointed out in an article about the failure of the RBS connection before reaching the plastic flexural capacity (Han *et al.* 2009), and then they presented equations for the accurate calculation of the flexural strength of the reduced section to form the plastic hinge. In addition, they expressed the design equations for the moment resistance of RBS connection but they did not pay attention to the structural lateral system. In 2009, Kyoung Sun Moon studied braced tube frame system and offered stiffness based design, but did not mention the type and performance of the connection, as well as its approach to 40 to 80 floors buildings. Due to the fact that the previous researches have not investigated the performance of the RBS connection in tall buildings with braced tube frame system, this article studies the performance of connection in tall buildings with the above-mentioned systems. As a result, the effect of the presence of RBS on energy absorption ductility of the structure is investigated (Shariati *et al.* 2012c, Shariati *et al.* 2013, Shariati *et al.* 2014, Shariati *et al.* 2016, Shariati *et al.* 2017, Shariati *et al.* 2018, Toghroli *et al.* 2018a, Toghroli *et al.* 2018b, Zandi *et al.* 2018, Ziaei-Nia *et al.* 2018, Shariati *et al*. 2020).

2. Investigation method

In this research, three tall buildings in height ranges of 20, 25 and 30 floors were modelled and designed by SAP2000 software, and then a frame in each building was modelled in PERFORM-3D software under two RBS-free system and RBS-based system. Nonlinear time history dynamic analysis is used for each frame under Manjil, Tabas and Northridge excitations.

3. Modelling

In modelling of tall buildings, the floor plan type is used as shown in Fig. 2, the height of all floors is 3.6 meters and the height of the pent is 2.5 meters. The usage of buildings is residential and their construction site is in Tehran. Tehran is considered to be a relatively high seismic zone with a

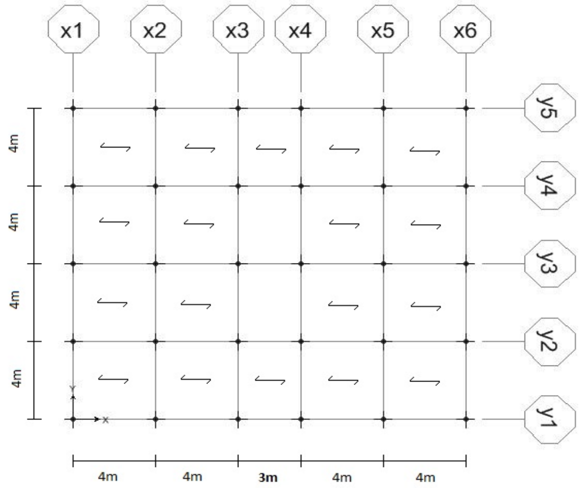

Fig. 2 Typical floor plan of the tall buildings

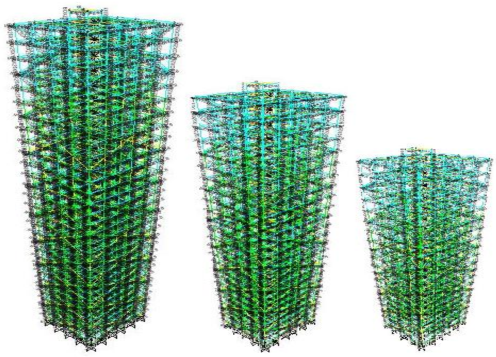

Fig. 3 The 3 modeled tall buildings with braced tube frame system

Table 1 Steel property

M = 800 Kg/m^3	Mass per Volume
W = 7850 Kg/m^3	Weight per Volume
E = 2.1x 106 Kg/cm^2	Elastic Modulous
υ = 0.3	Poisson's Ratio
Fy = 2400 Kg/cm^2	Yeilding stress
Fu = 3600 Kg/cm^2	Ultimate stress

maximum design acceleration equals to 0.35 g, and considering the classification of buildings according to importance, the models of this research are very important buildings with an importance factor equals to 1.2. The ground in the construction site is considered as type II, and in calculating the building seismic mass 20 percent of live loads were added to dead loads. The design of structures is in accordance with AISC codes and Allowable Stress Design (ASD) method. The basis of the seismic analysis is FEMA356 (Agency 2000).

The dead and the live load of each typical floor are 535 Kg/m^2 and 200 Kg/m^2 respectively. The dead and the live load of the top roof are 465 Kg/m^2 and 150 Kg/m^2 respectively, and the dead and the live loads of staircase are 700 Kg/m2 and 350 Kg/m2 respectively. The dead load of the surrounding walls in the typical floors is 465 Kg/m and in the top roof is 200 Kg/m, and a distributed 100 Kg/m^2 dead load is considered as a weight of partition walls in typical floors. As it is mentioned above, accelerograms of Manjil, Tabas and Northridge ground motions were used, and they were scaled according to the ASCE7-10 (Shariati *et al.* 2012a, Hosseinpour *et al.* 2018). In Table 2, the sections used in the tall buildings, which were obtained after design, were introduced. It should be noted that sections used in buildings are compact sections and there is no need to control local buckling of them (Shariati *et al.* 2012b, Shahabi *et al.* 2016, Tahmasbi *et al.* 2016).

The 3 tall buildings which are modelled and designed by SAP2000 software at three levels of 20, 25 and 30 floors are shown in Fig. 3.

Considering the performance of the connections in the braced tube frame system and also the fact that the frames

Table 2 Sections used in the models of the tall buildings

Box Columns	I Shape Beams	Box Braces
200×200×10 mm	IPE 180	200×200×10 mm
250×250×10 mm	IPE 200	250×250×10 mm
250×250×12 mm	IPE 300	250×250×15 mm
250×250×15 mm	I 300×150×8 mm	300×300×15 mm
300×300×15 mm		
300×300×20 mm		
350×350×15 mm		
350×350×20 mm		
350×350×25 mm		
400×400×20 mm		
400×400×25 mm		
400×400×30 mm		
450×450×20 mm		
450×450×25 mm		
450×450×30 mm		
450×450×35 mm		
500×500×30 mm		
500×500×35 mm		
500×500×40 mm		
550×550×40 mm		
550×550×45 mm		
600×600×45 mm		

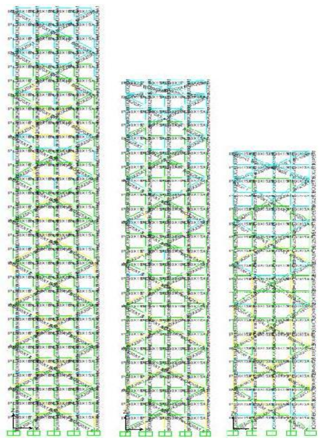

Fig. 4 The 3 studied models of tall buildings

have been constructed in the perimeter of the building, a two-dimensional analysis should be performed on one of the perimeter frames of the structure which have the characteristics of the braced tube frame system. Since the gravity load is one-sided, the outer frame X1 is selected in the direction Y which has gravity load on it. In Fig. 4, the studied frames are shown in three models.

The behaviour of the structural elements, according to their type of effort and the force-displacement diagram, is controlled by the displacement or controlled by the force. For the main members controlled by displacement, the displacement corresponding to the strength drop ratio to the displacement of the linear limit (e/g) is greater than 2, but the non-natural members are considered to be displacement controlled with any relation of e/g. Force-displacement diagram can indicate behaviour that is ductile, semi-ductile or brittle. In the ductile behaviour, the force-displacement diagram consists of four parts according to Fig. 5(a): 1. Linear elastic behaviour (OA branch) 2- Complete plastic behaviour or plastic behaviour with hardening (branch AB) 3- Strength drop (BC branch). 4. Plastic behaviour with softening (CD branch). In the semi-ductile behaviour, the force-displacement diagram consists of three parts according to Fig. 5(b): 1. Linear elastic behaviour (OA branch) 2- Complete plastic behaviour or plastic behaviour with hardening (AB branch) 3- Strength drop (BC branch), which the strength is sharply reduced, reaches zero at this stage. In this case, the e/g ratio must be greater than or equal to 2. In a brittle behaviour, the force-displacement diagram has a linear elastic part which then the strength is sharply reduced to zero, according to Fig. 5(c), The behaviour of the elements of the buildings studied in this article is ductile and thus, in the software modelling, the three lined diagrams with strength drop have been used.

In order to assign the ductile behaviour of Fig. 5(a) to the elements, the force-displacement diagram of FEMA356

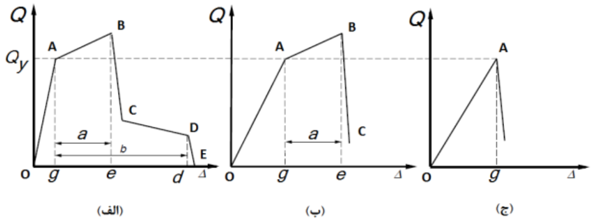

Fig. 5 Force-displacement diagrams of different element types

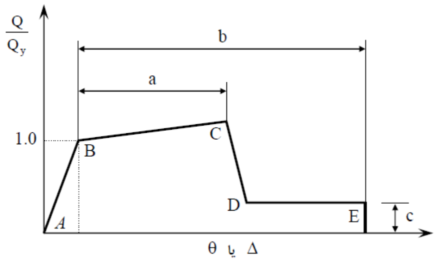

Fig. 6 The force-Displacement diagram of FEMA356 (Agency 2000)

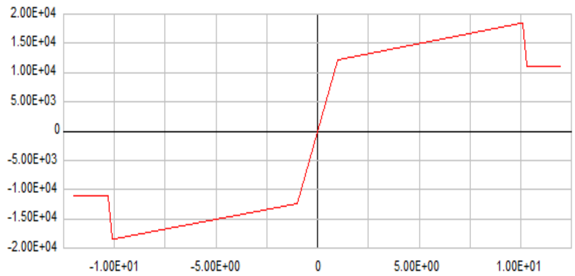

Fig. 7 The force-Displacement diagram introduced to the software

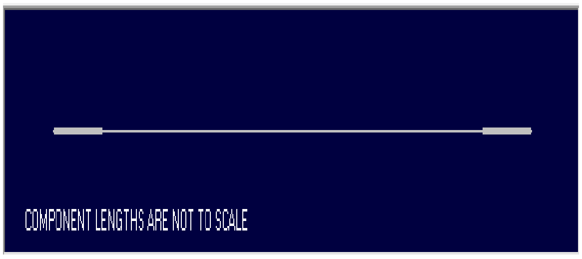

Fig. 8 Chord rotation model for RBS-free beams

has been applied, as shown in Fig. 6 and the modelling parameters must be assigned according to the three lined behaviour of the model elements. In this diagram, the horizontal axis represents displacement and the vertical axis represents force. Of course, the values of a, b and c shown in Fig. 6, along with other parameters required for modelling, should be derived from the tables of the FEMA356 code (Agency 2000).

Finally, after the required information was extracted and introduced to the software, the behaviour of the elements was shaped in Fig. 7.

For RBS-free beams, the chord rotation model was used. The model consists of two rigid ends on both sides and the FEMA Beam which its model has shown in Fig. 8. One of the important FEMA Beam element features is the automatic assignment of bending plastic hinge to the beams (Perform 2006).

The plastic hinge model is the best model for beams which their inelastic behaviour is limited in certain situations, such as beams with reduced sections. The RBS beam is shown in Fig. 9 (Perform 2006).

Thus, in the RBS beam, a plastic hinge model was used and shown in Fig. 10. Each end of this beam consists of

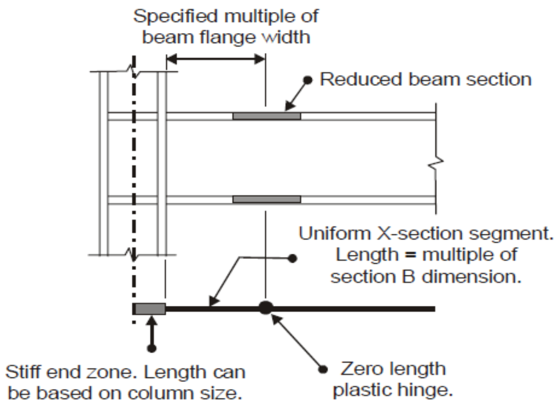

Fig. 9 RBS beam (Ellingwood 1980)

Fig. 10 Plastic hinge model for RBS beams

Fig. 11 The model of column

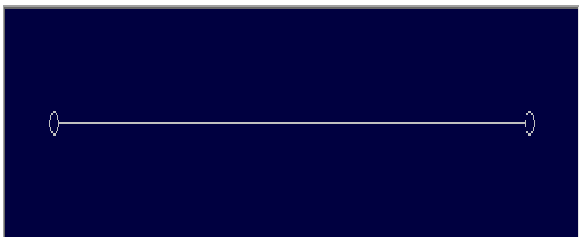

Fig. 12 The model of brace

three parts: First, a rigid area extending from the end of the joint to the outer surface of the column, second, a uniform section with variable length extending from the outer surface of the column to the RBS centre and third, a plastic hinge with a length of zero for introducing the RBS (Perform 2006).

It should be noted that in the modelling of the plastic hinge instead of RBS, the RBS modeling parameters must be calculated in accordance with the FEMA356 code tables and assigned to the plastic hinge with zero length.

As shown in Fig. 11, the model of the columns is consisting of two ridge areas at the top and bottom of the column. One of the important FEMA Column element features is the automatic assignment of the axial-bending plastic hinge to the columns (Perform 2006).

Different elements can be used to model the braces, but with the use of FEMA elements in beam and column modelling, the FEMA element is also used in braces. Of course, it should be noted that PERFORM-3D software does not directly contain the elements of the brace and should use beam or column elements instead to model the

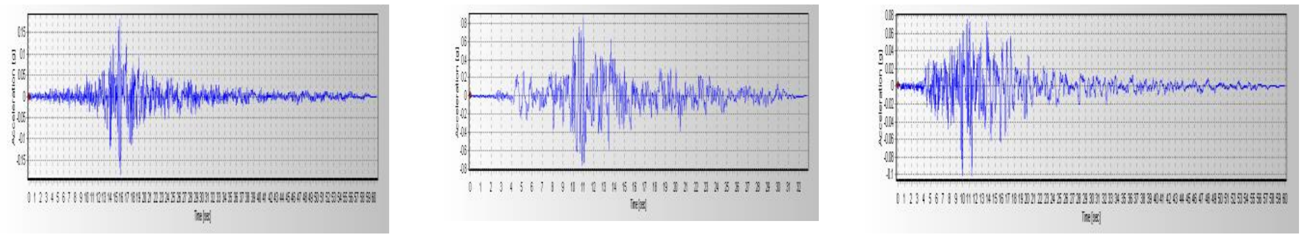

(a) Longitudinal component of Manjil earthquake (b) Transverse component of Tabas earthquake (c) Longitudinal component of Northridge earthquake

Fig. 13 The used component of (a) Manjil, (b) Tabas, and (c) Northridge earthquakes

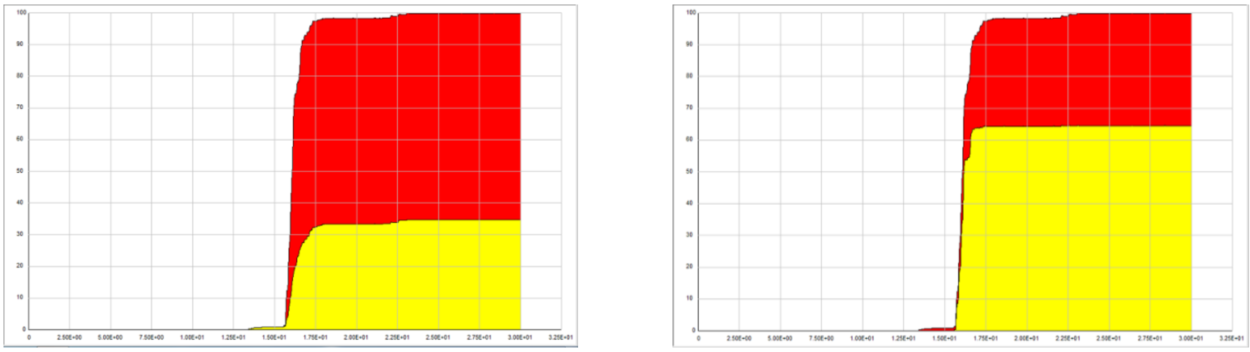

(a) The model without RBS connection (b) The model with RBS connection

Fig. 14 The absorbed energy under Manjil earthquake record by the beams of 20-story building a) Without RBS connection and b) With RBS connection

brace. In the beam element, there is no axial force and the bending moment is very high, which does not match the behaviour of braces. Therefore, due to the presence of axial force and the absence of bending moment in the braces, the FEMA Column element is preferred for modelling.

Of course, in order to prevent the moment in the brace, the start and the end of it are pinned and the end release is done. Thus, the brace model consists of two hinges at the two ends and FEMA Column sections, which is shown in Fig. 12 (Perform 2006) how it is modelled (Perform 2006).

For time history analysis, the load combination of 1.1(DL + LL), which is the most critical form of load combinations, has been used. Due to the fact that three-dimensional design was used in the tall buildings, the earthquake ground motion pairs were used, but due to the two-dimensional analysis, only one component of each record is needed. In this regard, the component used has bigger peak ground acceleration (PGA). Thus, the longitudinal component of the Manjil earthquake acceleration, the transverse component of the Tabas earthquake acceleration, and the longitudinal component of the Northridge earthquake acceleration are introduced to the software for seismic analysis. Also, for ease of analysis, 30 seconds of the record of each earthquake has been given to the software. Fig. 13 shows the accelerograms used.

Three levels of performance are introduced as Level 1 for Immediate Occupancy (IO), Level 2 for Life Safety (LS) and Level 3 for Collapse Prevention (CP) to the software, which is in accordance with the performance levels defined in the FEMA356 code. Two types of damping are defined as Rayleigh damping and Modal damping in models.

4. The result of seismic analysis

Depending on the severity and duration of the earthquake, the earthquake will cause structural displacement, which is associated with energy storage in the elements. Of course, as long as the displacements are small and in the linear range, it is reversible and the stored energy will be eliminated at the end of the earthquake. But with the entry of members into a nonlinear range, part of the stored energy is irreversible, which in turn causes permanent deformation in the members. In other words, this energy is stored in the form of material deformation.

One feature of the PERFORM-3D software is displaying the absorbed energy by the group of elements. In this way, the contribution of each group of elements of the beam, column and brace can be seen from the energy absorbed in each earthquake event. Also, the total energy absorbed or lost by the structure can also be studied. In the charts of energy absorption, the red colour represents all of the energy absorbed by the structure and the yellow colour indicates the contribution of the element group in its absorption. The horizontal axis indicates the time and the vertical axis represents the energy absorption percentage. In Figs. 14 to 16, the contribution of all beams, columns, and braces in energy absorbed by the total structural elements is

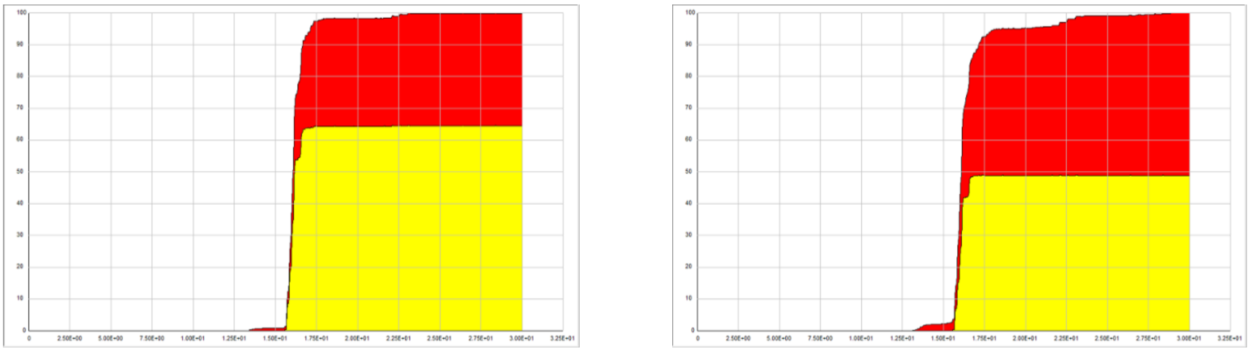

(a) The model without RBS connection (b) The model with RBS connection

Fig. 15 The absorbed energy under Manjil earthquake record by the columns of 20-story building (a) Without RBS connection and (b) With RBS connection

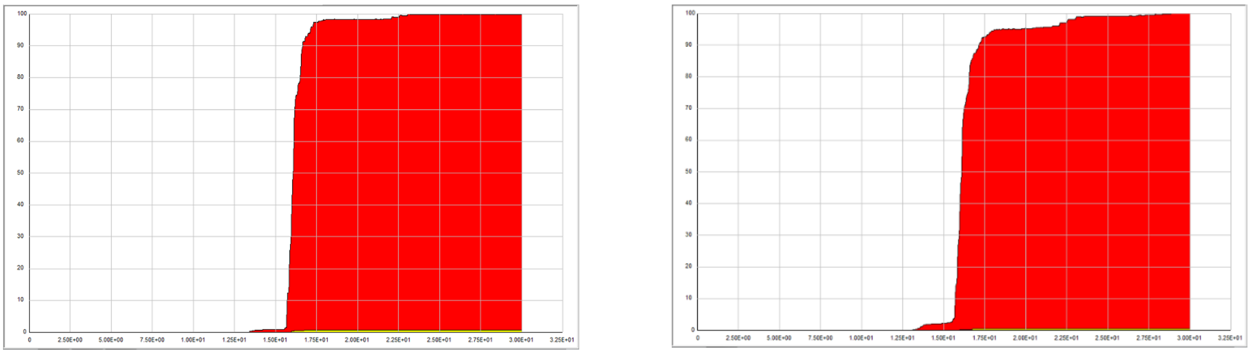

(a) The model without RBS connection (b) The model with RBS connection

Fig. 16 The absorbed energy under Manjil earthquake record by the braces of 20-story building

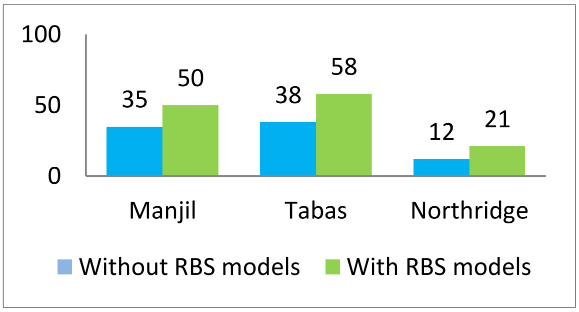

Fig. 17 The absorbed energy of beams in 20-story building

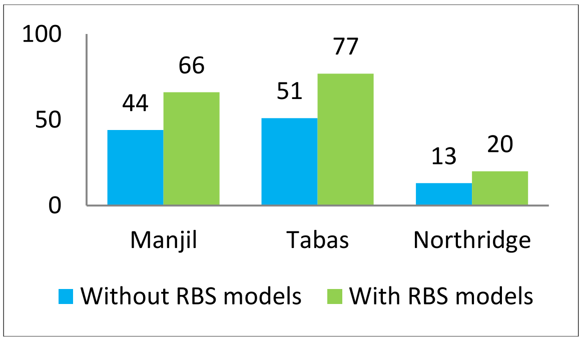

Fig. 18 The absorbed energy of beams in 25-story building

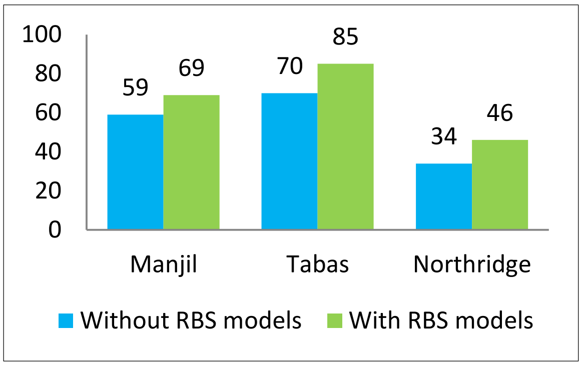

Fig. 19 The absorbed energy of beams in 30-story building

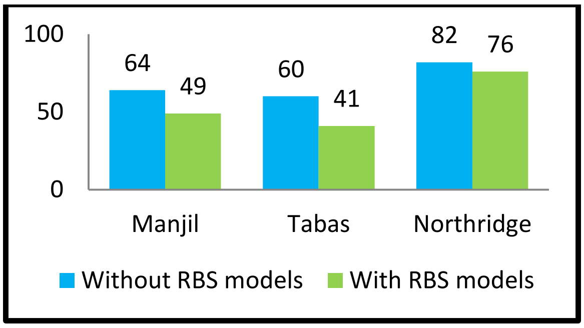

Fig. 20 The absorbed energy of columns in 20-story building

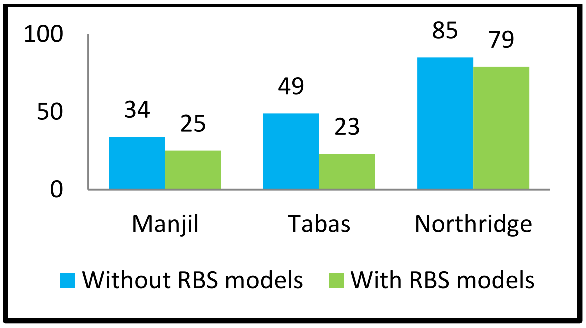

Fig. 21 The absorbed energy of columns in 25-story building

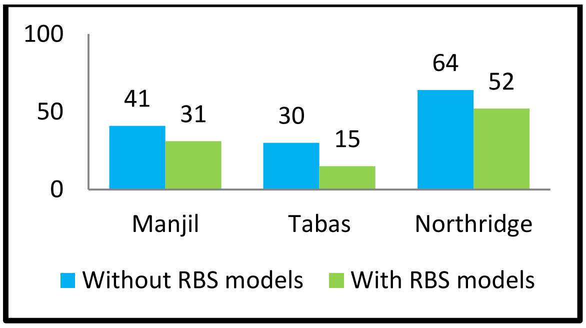

Fig. 22 The absorbed energy of columns in 30-story building

observed in two structural cases of with and without RBS connection. Of course, the Figures shown in this section relates only to the elements of the beam, the columns and braces of the structure of the 20-story structure, under the

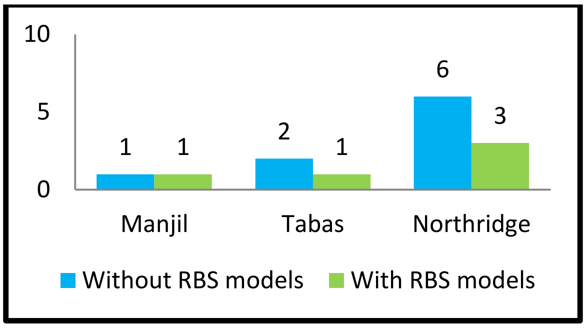

Fig. 23 The absorbed energy of braces in 20-story building

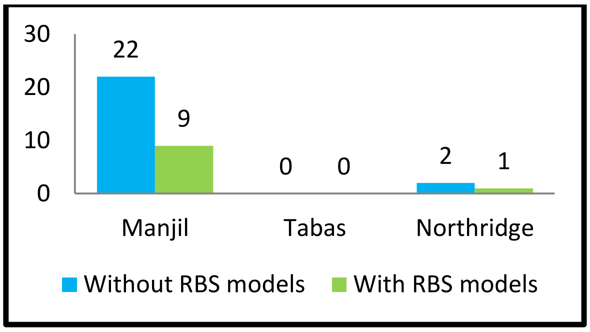

Fig. 24 The absorbed energy of braces in 25-story building

Manjil earthquake record.

As shown in Figs. 14 to 16, the beams with RBS connection have a higher energy level than the RBS-free beams; however, the columns in the model with RBS have lower energy level than the column without RBS. Braces also have a similar status to the columns energy absorption, but due to the low participation of the braces elements in comparison to the column in the absorption of energy and low energy levels in them, this is not a significant decrease. Before discussing this issue, the energy absorbed by the element groups is being discussed again.

Table 3 The absorbed energy increase percentage in the beams in the presence of RBS connection

Model	Manjil	Tabas	Northridge
20-story	15	20	9
25-story	22	26	7
30-story	10	15	12

Table 4 The absorbed energy decrease percentage in the columns in the presence of RBS connection

Model	Manjil	Tabas	Northridge
20-story	15	19	6
25-story	9	26	6
30-story	10	15	12

This time, bar graphs are used for better understanding. In the diagrams below, the horizontal axis indicating the earthquake occurrence and the vertical axis represents the absorbed energy percentage. Figs. 17-19 show the diagram of energy absorbed in the three structures of 20, 25 and 30 floors under the record of three earthquakes.

The diagrams shown above and the information in Table 3 indicate that in every structure and under any records, the level of energy absorbed by the beams increases significantly with the presence of RBS. In justifying this, it can be said that reducing the cross section of the beams at the location of the RBS causes a reduction in their stiffness. On the other hand, the stiffness and ductility are inversely related to each other, and as a result of the reduction of stiffness, it increases the ductility, and this increases the potential of the beams in absorbing and damping energy, and increases the contribution of beams in the absorption of input energy to the structure. Thus, with the presence of RBS connection in the structure the stiffness of the beams decreases and as a result, their ductility increases; hence a greater part of the input energy to the structure enters the beams and is stored in them by creating more displacement in the beams. In Figs. 20 to 22, the performance of the columns of the three models is compared to energy absorption under the three earthquake records.

It can be seen from the above diagrams as well as Table 4 that the energy absorbed by the column elements in the models with the RBS connection is significantly reduced compared to the structure without RBS connection, which is because the presence of RBS in the structure led to a larger portion of the total energy allocates to the beam elements

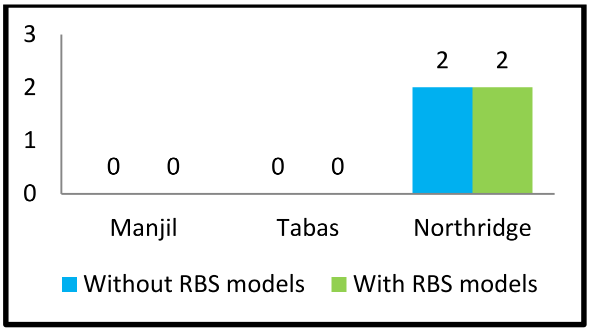

Fig. 25 The absorbed energy of braces in 30-story building

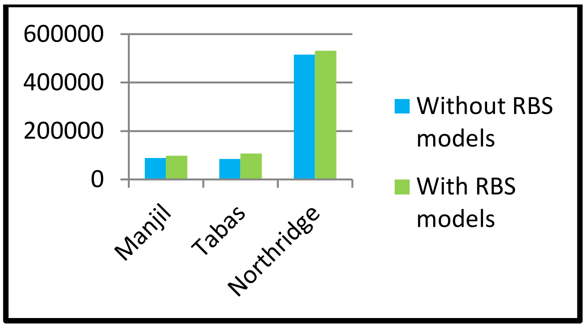

Fig. 26 The total amount absorbed energy in 20-story building

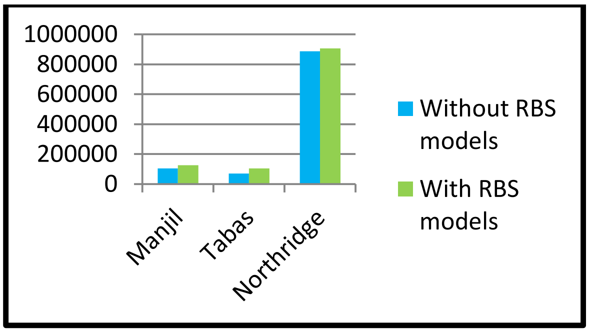

Fig. 27 The total amount absorbed energy in 25-story building

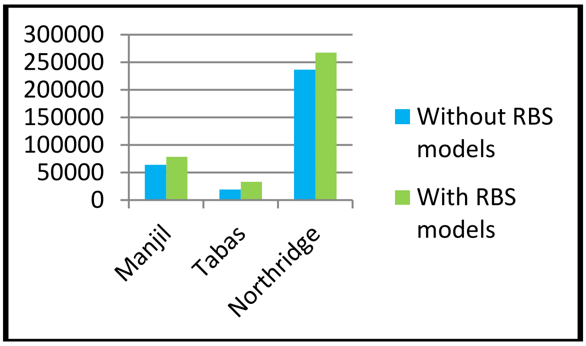

Fig. 28 The total amount absorbed energy in 30-story building

and with the greater contribution of beams to energy depletion, the contribution of columns to energy losses decreases significantly. Thus, the energy absorbed in the structural columns with RBS connection is associated with a decrease. In Figs. 23 to 25, the braces elements in the three tall structures under the three records are discussed.

In the parts of the charts, which there are a zero number, the absorbed energy level in the brace elements is less than 1 percent, which is approximated to zero. But there is still a decline in energy levels.

The above charts related to energy absorption in the brace elements and Table 5 illustrates what is seen in the column. The existence of an RBS connection has led to a greater contribution of input energy, to beams, and a reduction in the contribution of columns and braces to energy absorption; but due to the low contribution of the braces in energy depletion and the low energy absorbed in them in comparison to the beams and columns, this decrease is not significant.

In the case of energy absorption in the structure, the effect of the RBS connection can also be studied in a different way, the performance of this connection based on the total energy absorbed by the structure. To better understand this issue, the energy absorbed by the RBS-free structure and the energy absorbed by the RBS structure are compared. Figs. 26 to 28 show the total energy absorbed in two with and without RBS structures. The horizontal axis is the earthquake occurrence and the vertical axis is the total amount of energy absorbed in kilograms of force per meter. It is worth noting that this energy level is derived from 30 seconds of each record, but it is not an error to do the comparisons, and the answer is acceptable.

Table 4 The absorbed energy decrease percentage in the columns in the presence of RBS connection

Model	Manjil	Tabas	Northridge
20-story	15	19	6
25-story	9	26	6
30-story	10	15	12

Table 5 The absorbed energy decrease percentage in the braces in the presence of RBS connection

Model	Manjil	Tabas	Northridge
20-story	Less than 1	1	3
25-story	13	Less than 1	1
30-story	Less than 1	Less than 1	Less than 1

Table 6 The total input energy increase percentage in the presence of RBS connection

Model	Manjil	Tabas	Northridge
20-story	10.2	27	3
25-story	19.6	50.6	5
30-story	22.9	75	12.9

Regarding the above charts about the total input energy absorbed and the information in Table 6, the presence of RBS can increase the total amount of energy input to the structure in all models and all records, which is due to the reduction of the stiffness of the beams because of the decrease in the cross section at the RBS connection point. Reducing the stiffness of the beams reduces the stiffness of the structure and, consequently, increases its ductility. As the ductility of the structure increases, the total input energy to it also increases. Of course, according to the diagrams of Figs. 26 to 28 and Table 6, it can be seen that as the height of the structure increases, the difference in total energy input to the structure between the two with and without RBS models increases. In Fig. 29, this is clearly shown in which the horizontal axis represents the earthquake occurrence and the vertical axis indicating the percentage increase in the total energy input to the system with the presence of RBS in the structure.

Thus, from the 20-story structure to the 30-story structure, the presence of the RBS connection increases the total energy input to the structure by a higher rate. To explain this, it can be said that the RBS connection increases the ductility of the beams by decreases the stiffness of the beams. By increasing the height and the number of floors, the number of elements of the beam that reaches a higher ductility is increased. In other words, at higher altitudes, the number of more ductile elements of the beams is involved in energy absorption. As a result of greater participation, the ductility of the structural associates with a greater rate of increase; thus, the total energy input to the structure increases with increasing the number of floors. This indicates the positive effect of the RBS connection at high altitude and suggests that in higher structures, the higher the height, the greater the efficiency of the RBS connection in the energy absorption and the formation of the ductility which is necessary for the system and is very useful.

5. Conclusions

In this paper, the effect of reduced beam section (RBS) connection on energy absorption in tall buildings with braced tube frame systems has been investigated. For this purpose, nonlinear time history dynamic analysis was used and three earthquake records of Manjil, Tabas and Northridge ground motion were selected and then scaled according to the ASCE7-10 code. Also, three tall buildings of 20, 25 and 30 floors were modelled and designed by SAP2000 software. One frame was selected from each of the buildings for modelling according to FEMA356 in PERFORM-3D software under two systems of with and without RBS. Following the seismic analysis of models, energy absorption in the elements and the entire structures of 20, 25 and 30 story buildings under two systems with a reduced connection is shown on the bar graphs and tables and the results of the comparison of the systems are expressed there. The results are summarized and suggestions are made to expand the research work.

By analysing the models, the presence of RBS in the structure reduced the stiffness of the beams and, as a result, increased their potential for energy absorption, which led to an increase in the energy absorbed in the beams compared to the models without RBS. Therefore, the contribution of columns and braces in reducing the energy input to the structure decreases. Also, the increase in the energy absorbed by the beams is due to the increase of their ductility and, therefore, the structural system became more ductile by deformation and rotation in the beams. Therefore, it makes the total energy input to the structure increase and the system to find the equilibrium and stability required against the forces that are caused by the earthquake with a better performance. On the other hand, with the reduction of the stiffness of the beam, the design principle of strong column- weak beam is strengthened and the probability of collapse in the beam is increased in comparison to the column, which will increase the life safety of the occupants. Also, with the increase in the number of structural floors, the beams, which became more ductile in the presence of the RBS connections, contributed with many more numbers to the energy absorption, resulting in a greater rate of increase in the ductility of structural system and input energy absorption.

The results are counted below one by one:

- The use of RBS connection increased the energy absorbed in the beams significantly, due to the reduction in the stiffness of the beams at the joints and the increase in their ductility. Subsequently, due to more rotation, the beams experienced more deformation during the earthquake, which provided the need for the system to ductility.
- The use of RBS connection in the structure has completely different behavior in the columns in contrast to the beams and reduces the absorbed energy level, due to the increase in the contribution of beams to the absorption of energy into the structure. By reducing the energy level of the columns, we see a decrease in the ductility of the columns. Reducing the deformation of the column with its increase in the beam and, of course, reducing the stiffness in the beam, strengthens the design principl of strong column-weak beam, and alleviates structural designers' concerns about the high ranges of displacement and the possibility of column collapse.
- Reducing the energy absorbed in the columns is desirable because it increases the stability of the structure against earthquake-induced forces. Due to the fact that this connection, by creating fewer displacements in the columns than before, makes these elements to apply less proportion of their ductility capacity and reserves it to counteract more intense forces.
- The braces, like the columns, by lowering the energy level, have contributed less in the absorbing of the total energy absorbed by the structure compared to the previous ones. Of course, the brace elements do not play an important role in energy absorption, and without the presence of this connection, they also have little involvement in energy absorption, but the low level of energy that was absorbed before the use of this connection has also been accompanied by a reduction. It should be noted that in this system, the main task of the overall braces is to strengthen the building and a large part of the energy from the earthquake is entering the elements of the beam and the column due to the rigidity of the joints.
- The presence of the RBS connection in the braced tube frame system in the tall buildings has increased the total energy input to the structure, since RBS connection reduces the stiffness of the beams at the joints, thereby reducing the overall stiffness of the system and increasing its ductility. By increasing the ductility of system, the potential of structure in energy absorption rises and the total energy absorbed increases. This can cause high-rise buildings at higher altitudes to absorb more energy from the earthquake, form a favourable ductility and maintain their stability well.
- The results show that with the increase in the height of tall buildings due to the participation of the more number of ductile elements in the absorption of input energy to the structure, the total input energy to the structure is also increased with a greater rate in the presence of RBS connection. This reflects the fact that the use of the RBS connection in higher buildings is more efficient in absorbing energy from the earthquake and, by absorbing more energy and creating a more suitable ductility in the building, its stability is ensured.

In the end, it is suggested that in the future studies on the effect of the RBS connection on structural other systems be conducted, and the results should be studied. Other seismic parameters can also be checked. Also after structural analysis with this connection, the structure is redesigned so that the effect of the presence of RBS connections can be considered in the possibility of reducing the cross-section of the used elements.

References

Agency, F.E.M. (2000), “Prestandard and commentary for the seismic rehabilitation of buildings”, American Society of Civil Engineers (ASCE).

Bazzaz, M., *et al.* (2015), “Evaluating the performance of OBS-CO in steel frames under monotonic load”, *Earthq. Struct.*, **8**(3), 697-710.

Ellingwood, B. (1980), Development of a probability based load criterion for American National Standard A58: Building code requirements for minimum design loads in buildings and other structures, US Department of Commerce, National Bureau of Standards.

Fan, H., *et al*. (2009), “Seismic analysis of the world’s tallest building”, J. *Constr. Steel Res*., **65**(5), 1206-1215. https://doi.org/10.1016/j.jcsr.2008.10.005.

Ghassemieh, M. and Kiani, J. (2013), “Seismic evaluation of reduced beam section frames considering connection flexibility”, *Struct. Des. Tall Spec. Build*., **22**(16), 1248-1269. https://doi.org/10.1002/tal.1003.

Han, S.W., e*t al*. (2009), “Design equations for moment strength of RBS-B connections”, *J. Constr. Steel Res*., **65**(5), 1087-1095. https://doi.org/10.1016/j.jcsr.2009.01.003.

Heydari, A. and Shariati, M. (2018), “Buckling analysis of tapered BDFGM nano-beam under variable axial compression resting on elastic medium", *Struct. Eng. Mech.*, **66**(6), 737-748. https://doi.org/10.12989/sem.2018.66.6.737.

Hosseinpour, E., *et al.* (2018), "Direct shear behavior of concrete filled hollow steel tube shear connector for slim-floor steel beams", *Steel Compos. Struct.*, **26**(4), 485-499. https://doi.org/10.12989/scs.2018.26.4.485.

Jeong, S.H. and Elnashai, A.S. (2006), "New three-dimensional damage index for RC buildings with planar irregularities", *J. Struct. Eng.*, **132**(9), 1482-1490. https://doi.org/10.1061/(ASCE)0733-9445(2006)132:9(1482).

Kassegne, S.K. (2007), "Development of a closed-form 3-D RBS beam finite element and associated case studies", *Eng. Struct.*, **29**(7), 1580-1595. https://doi.org/10.1016/j.engstruct.2006.09.010.

Khorami, M., *et al.* (2017a), "Seismic performance evaluation of buckling restrained braced frames (BRBF) using incremental nonlinear dynamic analysis method (IDA)", http://dx.doi.org/10.12989/eas.2017.13.6.531.

Khorami, M., *et al.* (2017b), "Evaluation of the seismic performance of special moment frames using incremental nonlinear dynamic analysis", *Struct. Eng. Mech.*, **63**(2), 259-268. http://dx.doi.org/10.12989/sem.2017.63.2.259.

Khorramian, K., *et al.* (2017), "Numerical analysis of tilted angle shear connectors in steel-concrete composite systems", *Steel Compos. Struct.*, **23**(1), 67-85. http://dx.doi.org/10.12989/scs.2017.23.1.67.

Li, D., *et al.* (2019), "Application of polymer, silica-fume and crushed rubber in the production of Pervious concrete", *Smart Struct. Syst.*, **23**(2)207.

Milovancevic, M., *et al.* (2019), "UML diagrams for dynamical monitoring of rail vehicles", *Physica A: Statistical Mechanics and its Applications*, 121169.

Perform, C. (2006), "3D: Nonlinear Analysis and Performance Assessment for 3D Structures, Version 4", Computers and Structures, Inc., Berkeley, California.

Sajedi, F. and Shariati, M. (2019), "Behavior study of NC and HSC RCCs confined by GRP casing and CFRP wrapping", *Steel Compos. Struct.*, **30**(5), 417-432. http://dx.doi.org/10.12989/scs.2019.30.5.417.

Shah, S., *et al.* (2016a), "State-of-the-art review on the design and performance of steel pallet rack connections", *Eng. Failure Anal.*, **66**, 240-258. https://doi.org/10.1016/j.engfailanal.2016.04.017.

Shah, S., *et al.* (2016b), "Behavior of steel pallet rack beam-to-column connections at elevated temperatures", *Thin-Wall. Struct.*, 1**06**, 471-483. https://doi.org/10.1016/j.tws.2016.05.021.

Shahabi, S., *et al.* (2016), "Numerical analysis of channel connectors under fire and a comparison of performance with different types of shear connectors subjected to fire", *Steel Compos. Struct.*, **20**(3), 651-669. http://dx.doi.org/10.12989/scs.2016.20.3.651.

Shariat, M., *et al.* (2018), "Computational Lagrangian Multiplier Method by using for optimization and sensitivity analysis of rectangular reinforced concrete beams", *Steel Compos. Struct.*, **29**(2), 243-256. http://dx.doi.org/10.12989/scs.2018.29.2.243.

Shariati, A., *et al.* (2012a), "Investigation of channel shear connectors for composite concrete and steel T-beam", *Int. J. Phys. Sci.*, **7**(11), 1828-1831. DOI: 10.5897/IJPS11.1604.

Shariati, M. (2008), Assessment of Building Using None-destructive Test Techniques (ultra Sonic Pulse Velocity and Schmidt Rebound Hammer), Universiti Putra Malaysia.

Shariati, M., e*t al.* (2019), "Application of waste tire rubber aggregate in porous concrete", *Smart Struct. Syst.*, **24**(4), 553-566. https://doi.org/10.12989/sss.2019.24.4.553.

Shariati, M., *et al*. (2012b), "Fatigue energy dissipation and failure analysis of channel shear connector embedded in the lightweight aggregate concrete in composite bridge girders", *Proceedings of the 5th international conference on engineering failure analysis*.

Shariati, M., *et al.* (2014), "Fatigue energy dissipation and failure analysis of angle shear connectors embedded in high strength concrete", *Eng. Fail. Anal.*, **41**, 124-134. https://doi.org/10.1016/j.engfailanal.2014.02.017.

Shariati, M., *et al.* (2016), "Behavior of V-shaped angle shear connectors: experimental and parametric study", *Mater. Struct.*, **49**(9), 3909-3926. https://doi.org/10.1617/s11527-015-0762-8.

Shariati, M., *et al.* (2012c), "Behaviour of C-shaped angle shear connectors under monotonic and fully reversed cyclic loading: An experimental study", *Mater. Design*, **41**, 67-73. https://doi.org/10.1016/j.matdes.2012.04.039.

Shariati, M., *et al.* (2013), "Comparison of behaviour between channel and angle shear connectors under monotonic and fully reversed cyclic loading", *Constr. Building Mater.*, **38**, 582-593. https://doi.org/10.1016/j.conbuildmat.2012.07.050.

Shariati, M., *et al*. (2018), "Experimental investigations on monotonic and cyclic behavior of steel pallet rack connections", *Eng. Fail. Anal.*, **85**, 149-166. tps://doi.org/10.1016/j.engfailanal.2017.08.014.

Shariati, M., *et al*. (2017), "Assessment of stiffened angle shear connector under monotonic and fully reversed cyclic loading", *Proceedings of the 5th International Conference on Advances in Civil, Structural and Mechanical Engineering - CSM 2017*, Zurich, Switzerland.

Shariati, M., *et al.* (2020), "A novel approach to predict shear strength of tilted angle connectors using artificial intelligence techniques", *Engineering with Computers*, 1-21. DOI: 10.1007/s00366-019-00930-x.

Shen, J., *et al.* (2000), "Seismic performance of steel moment frames with reduced beam sections", *Eng. Struct.*, **22**(8), 968-983. https://doi.org/10.1016/S0141-0296(99)00048-6.

Sun, F.F., *et al*. (2011), "Development of new-type buckling-restrained braces and their application in aseismic steel frameworks", *Adv. Struct. Eng.*, **14**(4), 717-730. https://doi.org/10.1260/1369-4332.14.4.717.

Tahmasbi, F., *et al*. (2016), "Shear capacity of C-shaped and L-shaped angle shear connectors", *PloS One*, **11**(8), e0156989. https://doi.org/10.1371/journal.pone.0156989.

Thai, C.H., *et al.* (2012), "Static, free vibration, and buckling analysis of laminated composite Reissner-Mindlin plates using NURBS-based isogeometric approach", *Int. J. Numer. Method. Eng*., **91**(6), 571-603. DOI: 10.1002/nme.4282.

Toghroli, A., *et al*. (2018a), "Evaluation of the parameters affecting the Schmidt rebound hammer reading using ANFIS method", *Comput. Concret*, **21**(5), 525-530. http://dx.doi.org/10.12989/cac.2016.21.5.525.

Toghroli, A., *et al*. (2018b), "Potential of soft computing approach for evaluating the factors affecting the capacity of steel–concrete composite beam", *J. Intel. Manufact.*, **29**(8), 1793-1801. https://doi.org/10.1007/s10845-016-1217-y.

Vafai, A., *et al*. (1995), "The use of single diagonal bracing in improvement of the lateral response of tall buildings", *Struct. Des. Tall Build.,* **4**(2), 115-126. https://doi.org/10.1002/tal.4320040203.

Yoo, J.H., *et al.* (2008), "Influence of connection design parameters on the seismic performance of braced frames", *J. Constr. Steel Res.*, **64**(6), 607-623. https://doi.org/10.1016/j.jcsr.2007.11.005.

Zandi, Y., *et al*. (2018), "Computational investigation of the comparative analysis of cylindrical barns subjected to earthquake", *Steel Compos. Struct.*, **28**(4), 439-447. https://doi.org/10.12989/scs.2018.28.4.439.

Ziaei-Nia, A., e*t al*. (2018), "Dynamic mix design optimization of high-performance concrete", *Steel Compos. Struct.*, **29**(1), 67-

75. https://doi.org/10.12989/scs.2018.29.1.067.

CC